DEPTH-OF-BURIAL AND DECOUPLING EXPLOSION EXPERIMENTS IN ISRAEL: NEAR-SOURCE AND NEAR-REGIONAL SEISMIC ENERGY GENERATION

Yefim Gitterman, Rami Hofstetter, and Vladimir Pinsky

Geophysical Institute of Israel

Sponsored by Air Force Research Laboratory

Contract F19628-03-C-0124

ABSTRACT

During the third year of the project, two source phenomenology experiments were conducted at Oron phosphate quarry in Northern Negev. A special complicated technology was used for the creation of large cavities (up to 3.5 m) at different depths (up to 63 m), and accommodation of large near-spherical charges of ANFO explosives.

A series of decoupled and fully coupled (reference) explosions with charges of 1240 kg in the cavities was conducted on July 17, 2006. Extensive observations in near-source zone and remote area demonstrated peculiar signal characteristics and energy generation features related to these specific decoupled seismic sources. S/P energy ratios and decoupling factors were estimated at local distances, matching roughly to theoretical conceptions.

The project central Depth-of-Burial (DOB) experimental series was conducted on January 2, 2007, and included three equal near-spherical charges of 4,200 kg at depths 26 m, 45 m and 59 m. The main objective of the experiment was to investigate relations between explosion depth and spectral/energetic/magnitude parameters of regional seismic phases. The design and configuration of the Oron DOB experiment were preferable in purity of conditions compared to the previous Balapan DOB experiment (1997): media homogeneity (all charges were placed in similar consolidated sediments), full containment and small separation (~200 m) of the explosions, charge scaled depths in the range of Nevada Test Site (NTS) nuclear tests. An important goal of our experiment was to get rid of the asymmetry effect caused by the difference of lithostatic pressures above and below the vertical lengthy cylinder explosive source, typical for borehole chemical explosions, and to study the generation of shear waves for about spherically symmetric sources, typical for nuclear tests.

Numerous good recordings of signals from all shots were obtained at portable near-source accelerometers and close-in 3C seismic stations, permanent local short period (SP) and broad band (BB) stations, and International Monitoring System (IMS) stations EIL and MMAI in Israel, and ASF in Jordan. An important effect observed for near-source accelerometer records was a clear trend of the signal peak amplitude and energy enhancement with the charge depth increase. This effect was accompanied by a significant signal frequency raise, providing empirical verification and estimation of decreasing seismic source size due to increase of overburden lithostatic pressure. Evidently, high frequencies of the radiated signal resulted in rapid attenuation of seismic energy with distance, a drastic drop of amplitude for deeper shots is clearly manifested already at distance of several km, and consequently a clear expected tendency of signal energy and magnitude reduction with depth is observed at regional distances. Analysis of seismic waveforms (in the broad band 1–20 Hz) at close local and regional distances (3.5–240 km) demonstrated a clear decrease of peak amplitude and energy for S-phase and corresponding S/P ratios for deeper shots. The frequency dependence of spectral amplitudes on shot depth was observed at most stations for the both phases: a decrease of amplitudes with increasing shot depth between about 1 and 10 Hz is converted to the opposite trend at higher frequencies ~10–20 Hz.

A special feature of Oron DOB experiment - the placement of the charges in boreholes, separated by only a few hundred meters, in order to eliminate variations in waveforms and travel times due to different propagation conditions—provided a good opportunity for a comparative location study. Using measured P onsets at the observation range and a local 1D velocity model, the three explosions were located by two procedures: the standard grid-search least square procedure (LSQR), and a new model-free robust “Grid-Sign” (GS) algorithm with essential advantage shown by the latter due to eliminating error of the unknown velocity model misfit.

OBJECTIVES

1) conducting of near-spherical explosions of special design at different depth, in homogeneous media, excluding all factors affecting radiated signals except of the DOB; and also partially decoupled shots;
2) quantifying the decoupling factor for these specific seismic sources, analysis of energy generation and partitioning into various regional phases (P and S).
3) estimation and analysis of relationship between explosion depth and spectral/energetic (magnitude) parameters of regional seismic signals.

RESEARCH ACCOMPLISHED

During the third year of the project, two source phenomenology explosion experiments were conducted at Oron phosphate quarry in Northern Negev (Figure 1). A special complicated blast design and technology were utilized, developed by Rotem Amfert Negev, Ltd., and Tamar Advanced Quarrying, Ltd., to provide near-spherical explosion sources. ANFO explosives were accommodated in large cavities (up to 3.5 m) at different depths (up to 63 m), created beforehand by a series of small shots in boreholes of a small diameter (6.5"), thus forming large near-spherical charges. This technique was used for the calibration Rotem 25-ton explosion in 2002 (Gitterman et al., 2002), where cavities of ~1 m size were created in holes at the depth ~15 m.

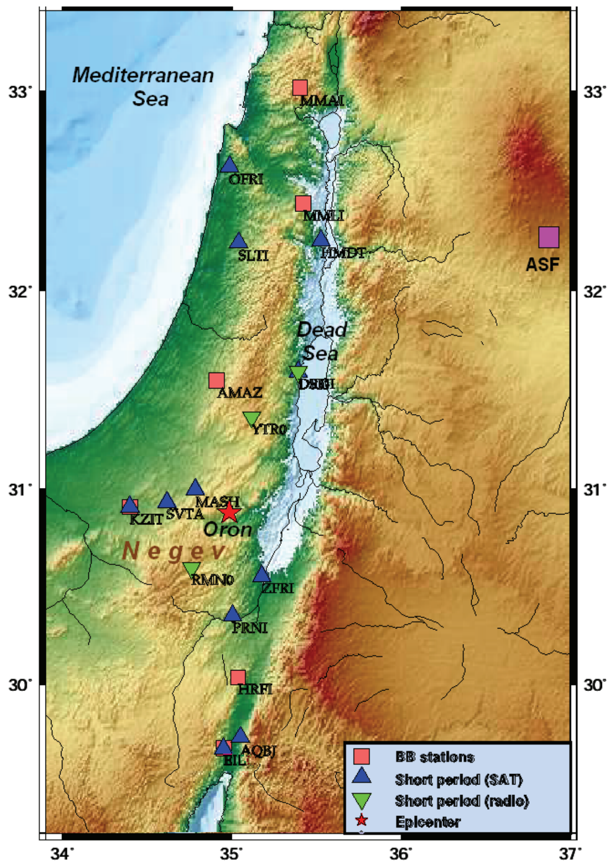

Figure 1. Explosion site and regional seismic stations that recorded signals.

Decoupling Experiment

A series of decoupled and fully coupled (reference) explosions with charges of 1,240 kg in the cavities was conducted on July 17, 2006 (Figure 2a). The spacing between the shots was 30–120 m. The idea and design of this experiment were initiated by special circumstances in preparations of the planned DOB experiment (Gitterman et al., 2006). Note that this "Decoupling" experiment was not quite pure, because all 3 shots were placed at different depths, and the cavity volume could be estimated rather approximately.

The site geology was presented by near-surface alluvium, and underlying consolidated marls and phosphates with similar mechanical properties and elastic velocities (Figure 2b), providing rock media homogeneity for all the sources. Different 3C observation systems were deployed at near-source distances: 9 accelerometers ETNA, range 100–700 m; 3 sensors BlastMateIII, 500–1000 m; 5 SP seismic stations L4C, 4–23 km. Extensive good-quality datasets obtained for all shots in near-source zone and remote area demonstrated peculiar signal characteristics and energy generation features related to these specific decoupled seismic sources. Very high signal frequencies accompanied by the highest peak accelerations were observed at all near-source distances for the decoupled Ex.2 (Figure 3). Possibly a smaller volume size of the seismic source, due to a larger depth (63 m) can contribute to this effect. However, it is problematic to explain a sharp rise of the radiated signal frequencies from 3–15 Hz to 30–40 Hz only by the doubled depth increase (as in the DOB experiment data, see below). A more reasonable guess (A. Dainty, pers. comm.) explains this effect by air-shock wave reverberations in the air-filled cavity. Considering the cavity maximal vertical dimension l_v~4 m, and the average shock wave velocity V~400 m/s, a rough estimation of the dominant reverberation frequency is $f_r = V/2l_r$ ~50 Hz, i.e., comparable to the observations. This phenomenon was modeled for cavity decoupled nuclear explosions in salt and tuff (Stevens et al., 1991); however, much higher reverberation frequencies (>100 Hz) were obtained.

Rapid attenuation of high-frequency seismic energy for Ex.2 resulted in minimal signal amplitudes already at the closest portable station at 4 km (Figure 4a) and at all regional stations (Figure 4b), and appropriate small local (duration) magnitude M_L=1.5, estimated by the Israel Seismic Network, compared to M_L=2.4 for the reference coupled Ex.3. Note very weak S-waves for Ex.2, compared to Ex.3.

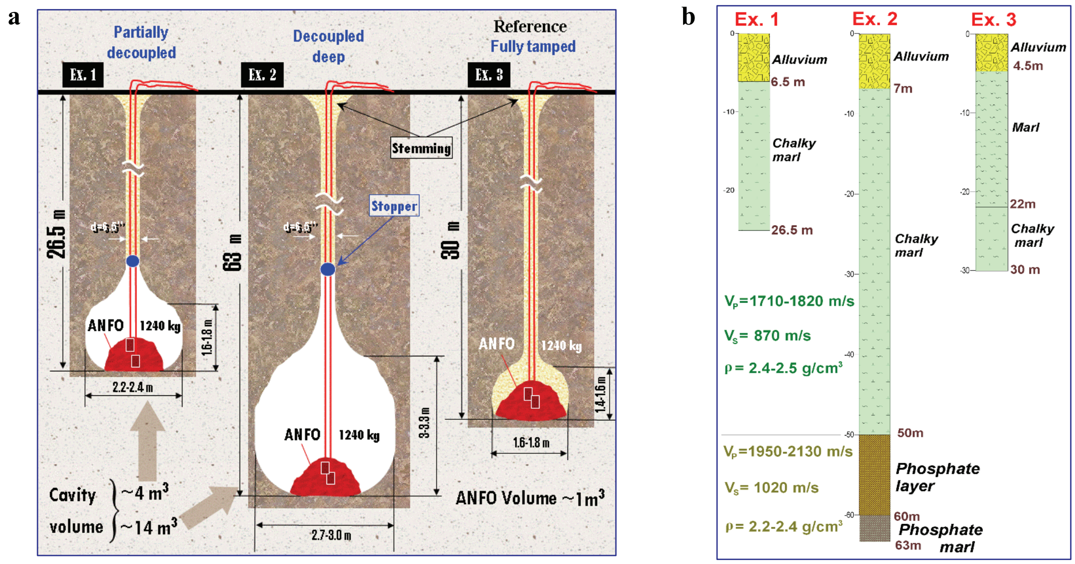

Figure 2. Design of the Decoupling experiment (a) and the site geology from the shot borehole drilling logs (b).

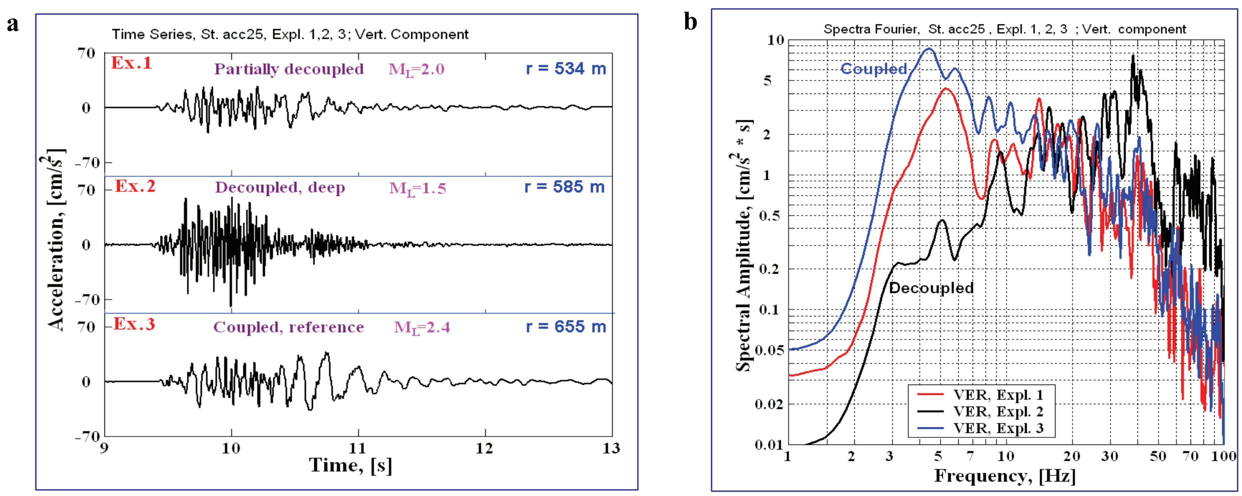

Figure 3. Vertical signal records (a) and spectra (b) at ~0.6 km (accelerometer ETNA). Local (duration) magnitudes M_L and epicentral distances are also shown.

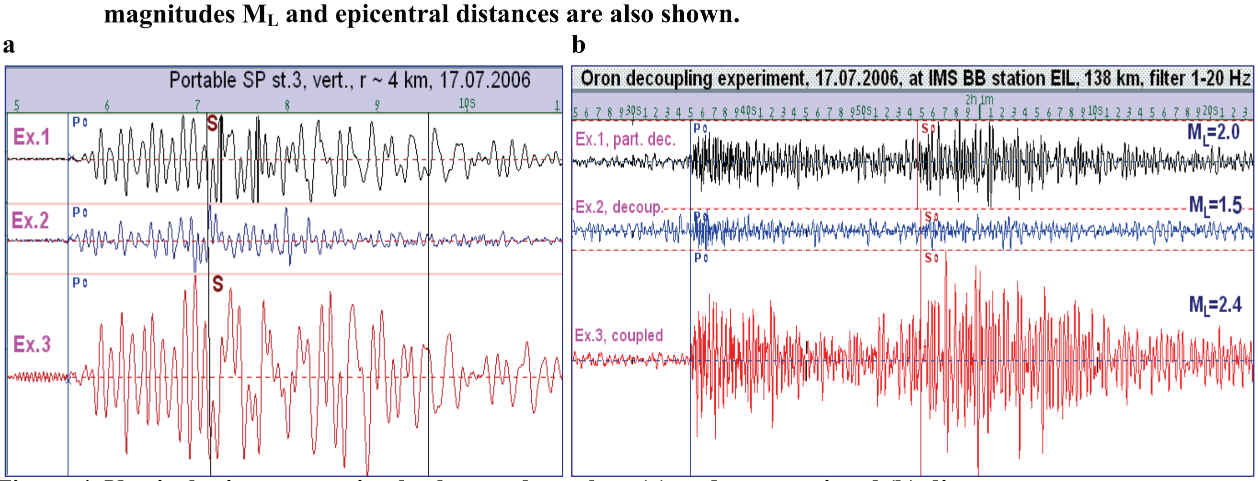

Figure 4. Vertical seismograms in absolute scale at close (a) and near-regional (b) distances.

We tried to estimate a Decoupling Factor (DF) as the ratio of peak (vertical) amplitude for the coupled (reference) shot (Ex.3) to the amplitude for a partially decoupled shot (Ex.1, Ex.2). We used vertical records of two SP (ZFRI, PRNI) and two BB (HRFI, EIL) stations in the distance range 40–140 km (Figure 5). We roughly estimated the cavity volume V as ~4 m^3 for Ex.1 and ~14 m^3 for Ex2 (see Figure 2a), and the TNT equivalent charge as W_{eq}~1000 kg (1,240 kg ANFO), then the Charge/Volume ratio W_{eq}/V (kg/m^3) was calculated as ~250 for Ex.1 and ~70 for Ex.2. The average DF values obtained (Figure 5b) fit predicted factors; however, they were calculated for granite (Stevens et al., 2003).

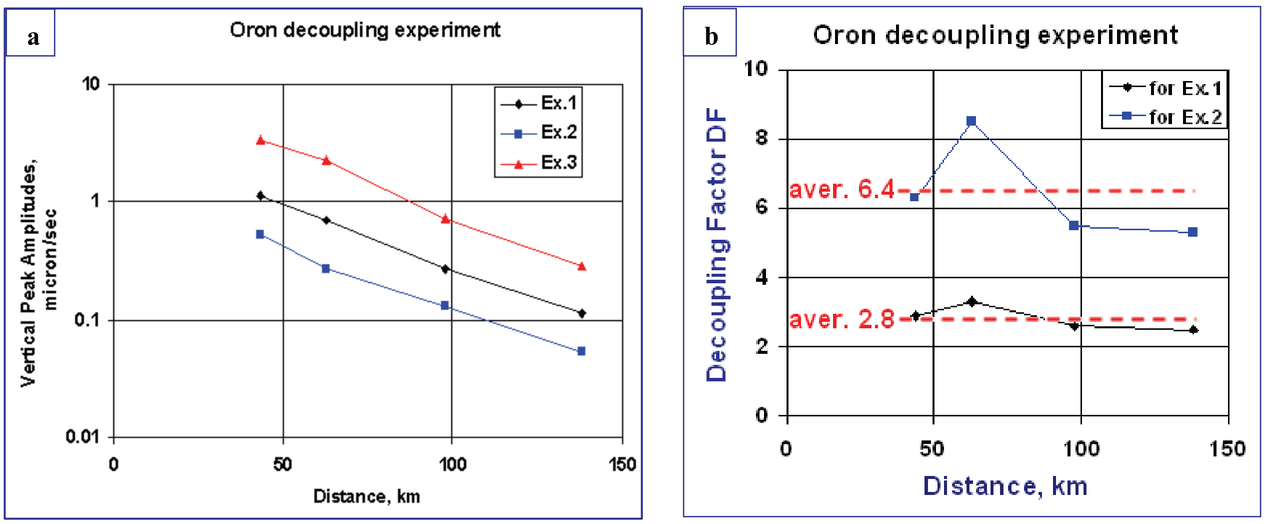

Figure 5. Signal peak amplitude (a) and Decoupling Factor (b) in a broad distance range for the partially decoupled explosions in soft sediment media.

We estimated seismic energy partition for the three explosions. For the selected five stations (a portable SP station at ~4 km was added) we calculated seismic energy for regional phases P, S (vertical component) in time windows T different for each station, but under condition Ts/Tp~1.5, and then S/P energy ratios (Figure 6). Obtained estimation results show that at all distances maximal S/P ratios are found for the coupled Ex.3, minimal S/P ratios—for the deep decoupled Ex.2.

Note that the twice larger shot depth for Ex.2 (compared to Ex.3) could result in smaller S-wave energy radiation (see below), and thus contribute together with the decoupling effect to the observed difference in S/P ratios.

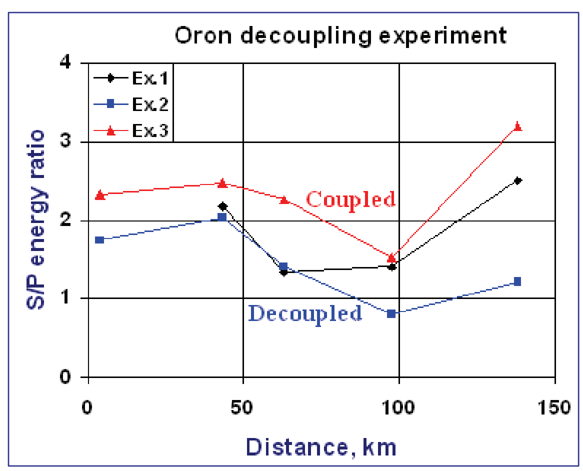

Figure 6. Energy partition estimation: S/P energy ratio for the Decoupling series shots.

Depth-of-Burial Experiment

The project central DOB series was conducted on Jan 2, 2007, and included three equal near-spherical charges of 4200 kg ANFO at depths 26 m, 45 m and 59 m, spacing between the shots was 200–300 m (Figure 7, Table 1). The main objective of the experiment was to investigate relations between explosion depth and spectral/energetic/magnitude parameters of regional seismic phases, especially S/P ratio. The site geology was presented by the same soft sediments with similar mechanical properties as for the nearby (~2.5 km away)

Decoupling explosion site (Figures 2b, 7), therefore rock media was homogeneous for all the sources. The charge weight was utmost maximal which provided full containment for all 3 shots: we observed a small ground surface uplifting on the video-record and thin cracks around the hole for the shallowest Ex.1, but no craters were found.

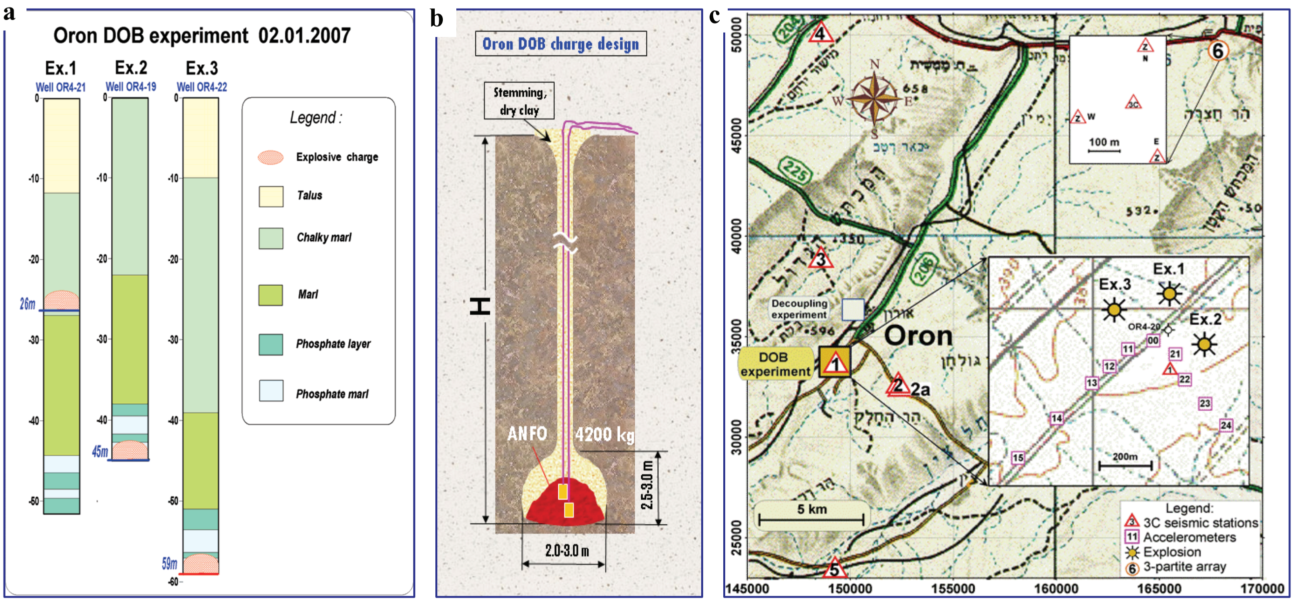

Figure 7. Geology of explosion boreholes from drilling logs (a); specific charge design providing large near-spherical seismic sources (b); location of the two experiment sites and portable stations, two insertions show detailed location of the tripartite array elements (st.6) and configuration of the explosion boreholes and accelerometers (c).

Tabel 1. Parameters of DOB Explosions

Ex. No.	Hole ID	Hole depth H, m	O.T. GMT	Local duration magnitude	Coord. (local)		Lat.	Long.
					X, km	Y, km		
1	OR4-21	26	09:31:12.317	2.7	149.294	34.058	30.89714	34.99353
2	OR4-19	45	10:01:13.442	2.6	149.428	33.858	30.89530	34.99498
3	OR4-22	59	10:30:31.276	2.5	149.082	33.994	30.89656	34.99133

Different 3C observation systems were deployed at near-source distances: 10 accelerometers ETNA, range 120–870 m; 4 SP seismic stations L4C, 3.5-16 km; a tripartite SP array (st.6) at 24 km deployed by Israel National Data Center (NDC) (Figure 7c). Extensive good quality datasets were obtained for all explosions from portable and permanent regional seismic stations, including IMS BB stations EIL, MMAI array, ASF, Jordan (Figure 1), in broad distance range 0.15–238 km. The records demonstrated peculiar signal characteristics and energy generation features related to these specific near-spherical seismic sources at different depths.

At near-source accelerograms, highest amplitudes are observed for the deepest Ex.3, though it was the weakest event with the minimal magnitude, estimated at regional distances (Table 1). A clear trend of peak amplitude and energy enhancement with the charge depth are found, with a simultaneous rise of signal frequencies. Sample vertical accelerograms for the closest (equidistant ACC00) and remotest (ACC15) stations and the whole signal amplitude spectra (Figure 8) show that the largest peak ground acceleration values for the Ex.3 are accompanied by high frequencies: maximal energy at 10-20 Hz and significant spectral peaks at higher frequencies up to 40–50 Hz, unlike the "shallow" Ex.1, with maximal energy at 3–14 Hz and a sharp drop at higher frequencies.

As early as r~3.5 km, the attenuation of high-frequency seismic energy results in minimal peak amplitudes and spectra for Ex.3 in the range 0.5-10 Hz, yet keeping maximal energy at higher frequencies (Figure 9). A drastic drop of amplitude for the deepest Ex.3 (compared to Ex.1) is clearly manifested at a continuous 1-hour record of closely located 3-component SP st.6 in the portable tripartite array (Figure 10). The well known reduction of signal energy and event magnitude with the source depth (e.g., Richards and Kim, 2005) is observed at all local and near-regional distances (Figure 11). Decrease of spectral amplitudes with increasing shot depth between about 1 and 10 Hz is converted to the opposite trend at higher frequencies ~10–20 Hz (Figures 9-11,b). Local (duration) magnitude M_L values for 3 DOB shots, averaged over several stations of Israel Seismic Network and plotted versus source depth, demonstrate linear relationship (Figure 12a). A similar correlation for analogous Balapan DOB experiment is plotted by utilizing energy class K values estimated from regional stations (Mikhailova et al., 2001) (Figure 12b).

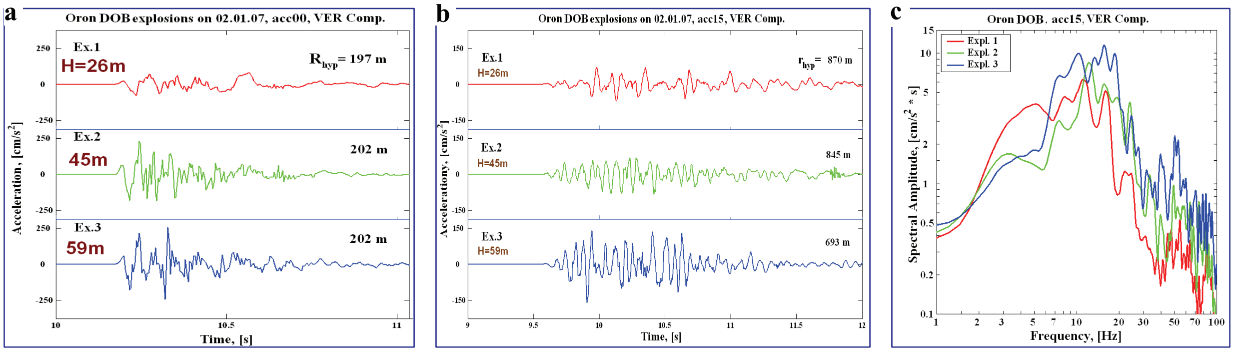

Figure 8. Vertical accelerograms at close station ACC00 equidistant from 3 DOB shots (a), and the remotest station ACC15 (b) and amplitude spectra (c). Hypocentral distances to the shots are shown.

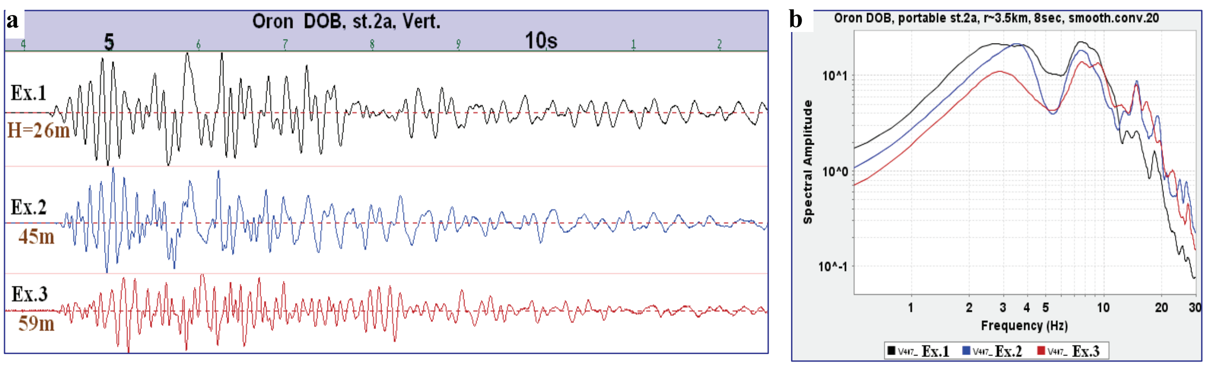

Figure 9. Vertical seismograms in absolute scale (a) and spectra of the whole signal (8 sec) (b) at the closest SP station at r~3.5 km. Note dominant energy for the deepest Ex.3 at high frequencies f >10 Hz.

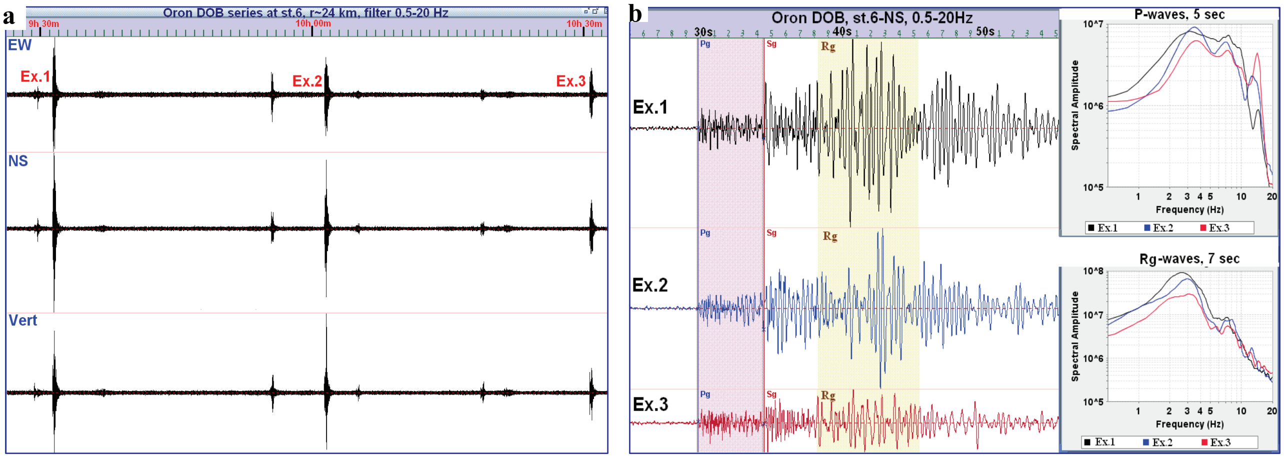

Figure 10. Close local recordings (in absolute scale) at the central 3C station of the SP tripartite array (St.6) at r~24 km: continuous 3C recording section of all 3 shots (a), NS records and spectra of P and Rg phases (b). A clear Rg onset is observed at vertical records (velocity ~2 km/s). Note a dominant spectral peak for Ex.3 at 13-15 Hz in P-phase which is not observed in Rg-phase.

To characterize better seismic energy generation for Oron DOB explosions we calculated the whole signal energy in the time domain recorded at 3C stations in the broad distance range (24–238 km), for different components – Vertical, Horizontal (the sum of energies for NS and EW components) and Vector (Figure 13). The Vertical energy shows a rather weak decrease with the source depth, while the Horizontal and Vector values drop more sharply.

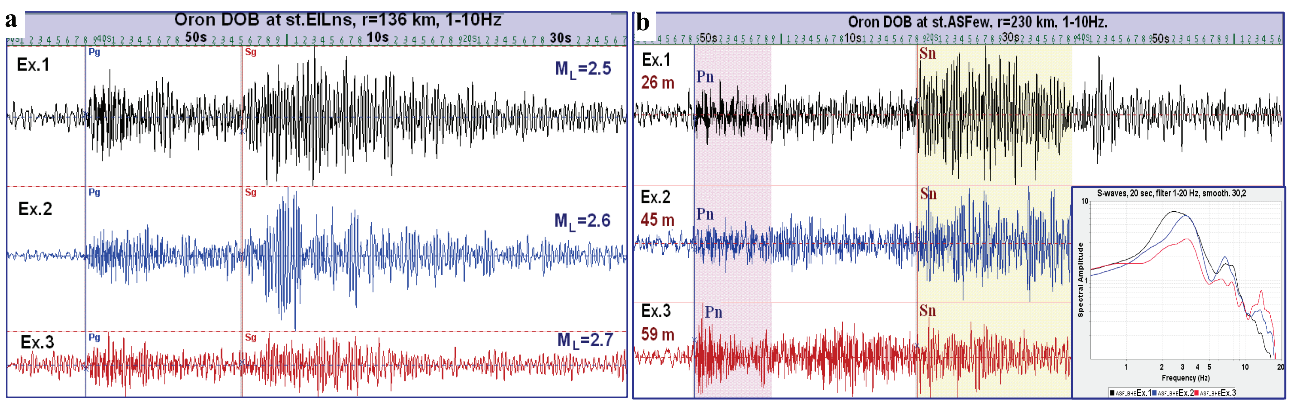

Figure 11. Horizontal seismograms (in absolute scale) at two IMS BB stations: EIL-NS (Radial) component (a), ASF-EW (~Transversal) component, windows for calculation spectra and spectral ratio are shown; conversion of spectra dominance for different shots at ~10 Hz is observed (b).

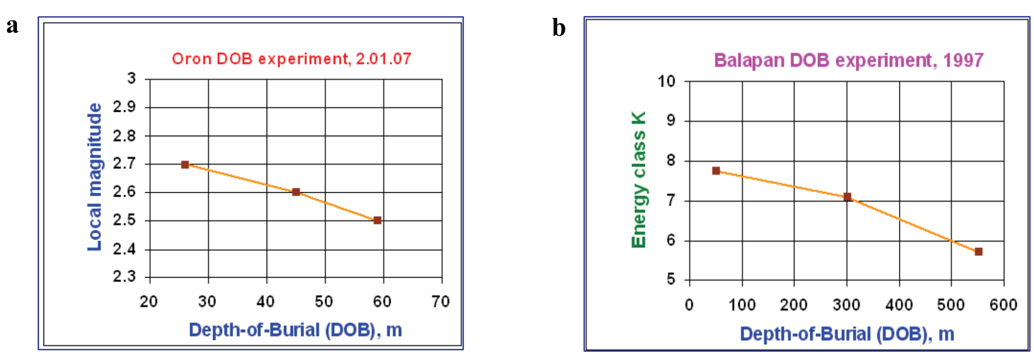

Figure 12. Magnitude versus source depth for two DOB experiments: local (duration) magnitude M_L at Oron (a) and Energy class K at Balapan (b).

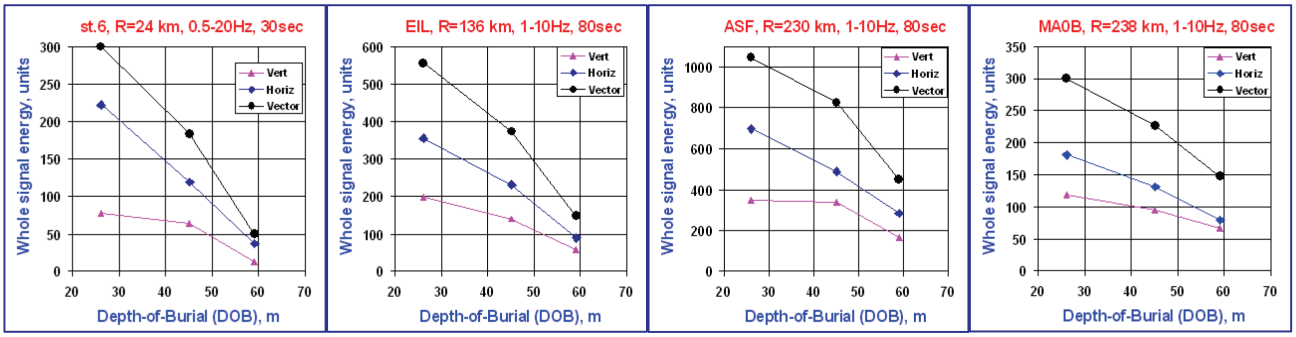

Figure 13. Seismic energy of the whole signal recorded at different components of several SP and BB stations versus source depth. Note different frequency range (filtering used) and signal duration.

Energy partition. As expected, at close local and near-regional distances observed amplitudes and energy of S-waves show significant and monotonous decrease with depth; while P-waves remain about constant or even increase (Figures 10b, 11). We evaluated relative excitation of P and S energy using 3C stations, based on identical propagation paths in the experiment, for differing depth sources. We calculated P/S spectral ratios for smoothed amplitude spectra of P and S phases and S/P energy ratios for different regional phases (Figures 14, 15). Different time windows were used depending on distance and reliable phase identification: equal short duration for clear phases Pg and Sg (4 sec), and Rg (7 sec) at the close SP st.6 (24 km) (see Figure 10b), and larger diverse windows for P-group (10 sec) and S-group (20 sec) at remote BB stations EIL, ASF and MMA0B (Figures 11, 14a), which include (Pn, Pg) and (Sn, Sg, Lg), because different P and S phases are not well separated at this distance range. Filtering was applied to close (0.5–20 Hz) and remote (1–10 Hz) records.

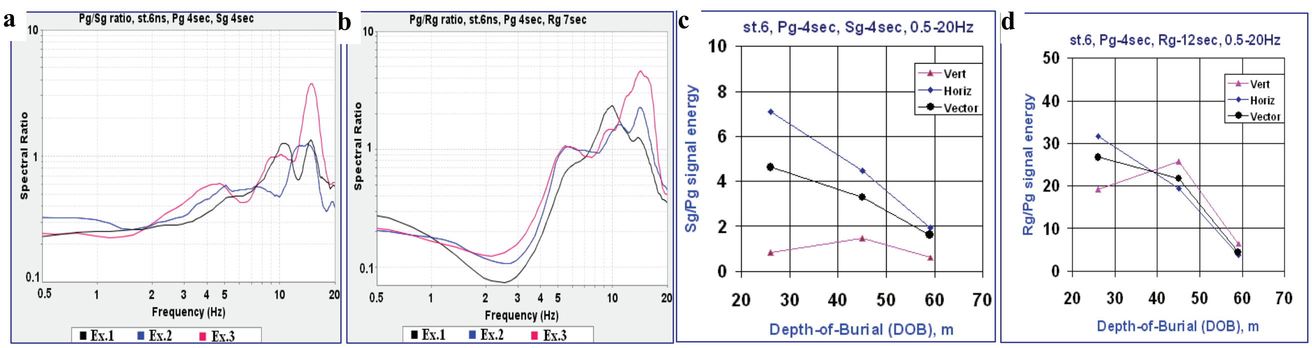

Figure 14. Energy partition at close local station st.6 (24 km): spectral ratios Pg/Sg (a) and Pg/Rg (b) suppose a weak dependence on source depth at 2–5 Hz; signal energy ratios Sg/Pg (c) and Rg/Pg (d) show an obvious decrease for deeper shots, especially for the Horizontal (EW+NS) component.

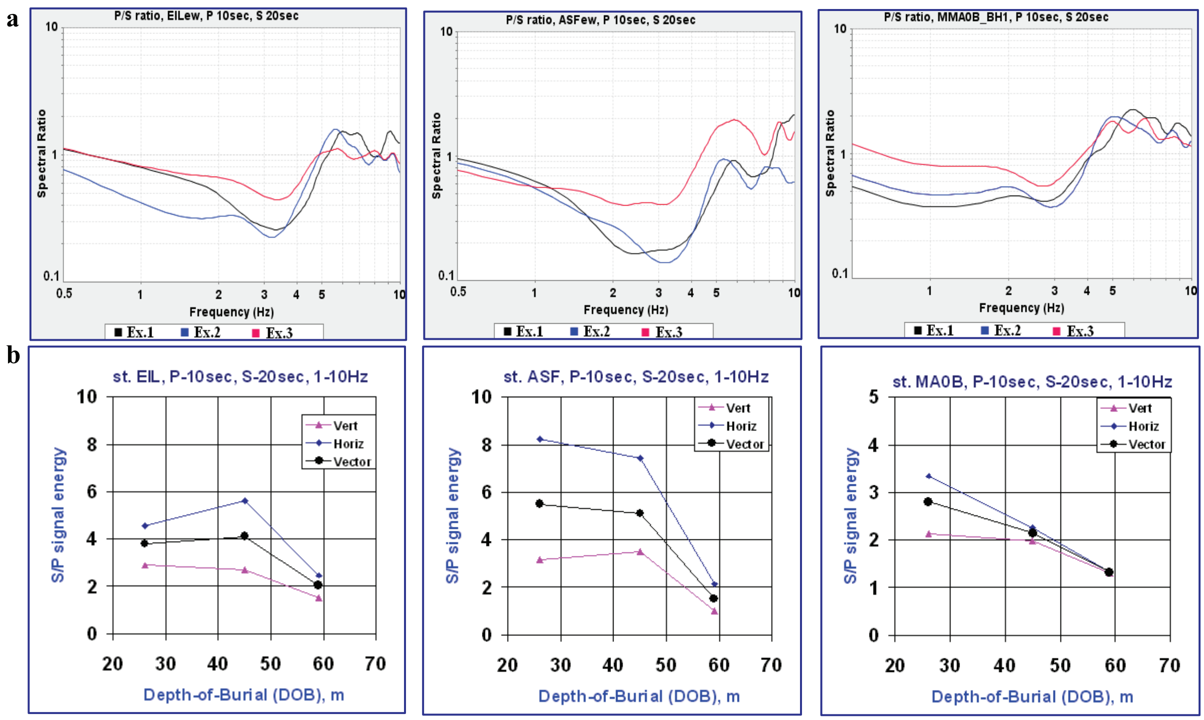

Figure 15. Energy partition at near-regional distances: spectral ratios P/S show decreased S-wave excitation for deeper shots in the range ~(0.5–8) Hz (a); signal energy ratios S/P decrease, in general, monotonous with depth (b).

Spectral ratios of Pg/Sg and Pg/Rg at close st.6 (24 km) (Figure 14a,b) show a weak dependence on DOB in a narrow band 2–5 Hz, whereas at near-regional distances a clear strong raise in the ratios is observed with increasing explosion depth, in the broader range about (0.5-8 Hz) (Figure 15a), as similar to results obtained for the Balapan DOB experiment (Mayers et al., 1999). Another characteristic of the radiated energy partition, the signal energy ratio S/P shows an obvious, monotonous (in-average) decrease for deeper shots, especially for the horizontal component.

Location analysis

A special feature of the Oron DOB experiment—the placement of the charges in holes, separated by only a few hundred meters, in order to eliminate variations in waveforms and travel times due to different propagation conditions—provided a good chance for a comparative location study. Using measured P onsets at the observation range and a local 1D velocity model, the three explosions were located by two procedures: the standard grid-search LSQR, and a new model-free robust GS algorithm (Pinsky, 2007) with the essential advantage shown by the latter due to eliminating the error of the unknown velocity model misfit (Figure 16, Table 2).

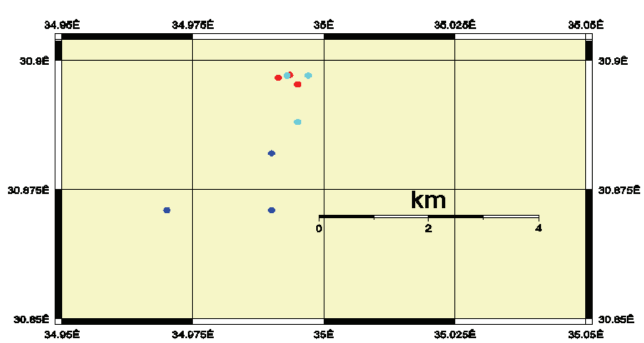

Table 2. Location error for three DOB explosions by different algorithms

#	Number of stations	GS	LSQR
		Error, km	Error, km
Ex.1	17	0.5	2.2
Ex.2	22	1.2	3.1
Ex.3	14	0.6	3.1

Figure 16. Location of the three DOB shots (● - Ground Truth) by the LSQR (●) and the GS (●) algorithms.

Discussion

The Oron Decoupling experiment was not pure, because the series shots were not placed at the same depth. However main features of the decoupling effect were observed and estimated, matching roughly to theoretical conceptions. The high frequencies (40–50 Hz), which we observed for near-source accelerograms of the decoupled shot, are lower than modeled for shock-wave reverberation (100–600 Hz) from nuclear sources (Stevens et al., 1991). It is explained by the fact that air-shock wave velocities for small chemical charges are much lower than for nuclear detonations with extremely high temperatures and pressures. The results also show that the utilized unique design of near-spherical sources can be used for the preparation of the full-scale, pure and cost-effective Decoupling Experiment.

The design and configuration of Oron DOB series were preferable in some conditions compared to the previous Balapan DOB experiment (Table 3). Initially we planned much deeper and afterwards—little smaller depths than realized, but after discussions (A. Dainty, pers. communication) we decided on the final charge depths in order to provide: 1) scaled depths in the range of NTS nuclear tests h=95-425 $m/kT^{1/3}$ (Springer et al., 2002); 2) full containment of all series shots.

Table 3. Comparison of design for two DOB experiments.

Parameter	1997 Balapan DOB	Oron DOB
Charge shape, aspect ratio (AR)	cylinder, L~34 m, AR~34	near-spherical, R~1-1.5m, AR~1
Scaled depth $h=Hc/W^{1/3}$, $m/kT^{1/3}$	113, 968, 1,823	167, 294, 387
Rock homogeneity	50-m shot—in sediments (shales), two others—in granites	Consolidated sediments: marls, chalky marls, phosphate marls
Explosion containment	50-m shot created a 40-m crater, for deeper shots the casing was ejected	all shots contained, 26-m shot created surface thin cracks
Spacing of the series shots	2.5–8.2 km	220–360 m (the same propagation even for close stations)

The increase of overburden lithostatic pressure with depth opposes to the opening and propagating of cracks and prevents non-linear deformations, thus squeezing the inelastic zone and decreasing seismic source size and volume in the model by Sharpe (1942), together with the volume expansion δV (Richards and Kim, 2005). Appropriate increased dominant frequencies of a radiated signal that we observed jointly with the near-source largest signal amplitudes, resulted in rapid attenuation of seismic energy with distance and minimal local magnitude.

For a long vertical source the decrease in pressure at shallow depth causes much stronger non-linear deformation above the explosion than below it, and this asymmetry results in the direct generation of shear waves, which would not be generated by spherical sources (Stevens, 2006). An important goal of our experiment was to get rid of the asymmetry effect caused by the difference of lithostatic pressures above and below the vertical lengthy cylinder explosive source, typical for borehole chemical explosions, and to study the generation of shear waves for about spherically symmetric sources, typical for nuclear tests. Nevertheless, we note that the observed on video-record small-amplitude surface uplifting for the shallowest Ex.1, H=26 m, may indicate an asymmetry effect caused by closeness to the surface, contributing to the generation of larger S-wave energy.

CONCLUSIONS AND RECOMMENDATIONS

- Oron experimental explosion series were conducted for the empirical modeling of decoupling effects and the relation between nuclear test depth and spectral/energetic parameters of regional seismic signals.
- A clear magnitude/energy reduction with depth was observed at regional distances, complemented by near-source observations of higher frequencies (and larger amplitude/energy) for deeper charges.
- S/P energy and spectral ratios and decoupling factors were estimated at close local and near-regional distances, roughly matching theoretical conceptions and known observations.
- The Oron DOB experiment with the original and adequate configuration and charge design was preferable in some conditions than the previous Balapan DOB (where detrimental factors affecting signals could not be excluded).
- Oron experiments demonstrated the feasibility of the utilized method of seismic source design for construction of near-spherical charges of different size (up to 10 tons) and at different depths (up to 70–80 m) and conducting broad-scale, low-cost experimental series: decoupling, DOB, variable charge weight.

ACKNOWLEDGEMENTS

Many individuals and organizations contributed to the success of the explosion experiments. We appreciate help of A. Dainty for useful discussions and information before and after the experiments. Special thanks to B. Hayoun of Tamar Ltd., Y. Levi and U. Yassur of Rotem Amfert Negev Ltd. for crucial a role in the preparation and conducting the special design explosions. Y. Ben-Horin of Israel NDC provided excellent records of the DOB experiment with a portable tripartite array. The GII staff performed technical support throughout the experiment, data processing and analysis; special thanks to U. Peled, M. Kalmanovich, N. Perelman, and A. Polozov.

REFERENCES

Gitterman, Y., V. Pinsky, A. Shapira, M. Ergin, D. Kalafat, G. Gurbuz, and K. Solomi (2002). Improvement in detection, location and identification of small events through joint data analysis by seismic stations in the Middle East/Eastern Mediterranean region, in *Proceedings of the 24th Seismic Research Review Nuclear Explosion Monitoring: Innovation and Integration,* LA-UR-02-5048, Vol. 1, pp. 271–282.

Gitterman, Y., R. Hofstetter, and V. Pinsky (2006). Source features and scaling of buried and surface experimental explosions in Israel, in *Proceedings of the 28th Seismic Research Review: Ground-Based Nuclear* Explosion Monitoring Technologies, LA-UR-06-5471, Vol. 1, pp. 597–606.

Mayers, S. C., W.R. Walter, K. Mayeda and L. Glenn (1999). Observations in support of Rg scatterieng as a source for explosion S waves: regional and local recordings of the 1997 Kazakhstan Depth of Burial Experiment, *Bull. Seism. Soc. Am.*.89: (2), 544–549.

Mikhailova, N., Germanova, T., Aristova, I. (2001). Estimation of energy and magnitude characteristics based on seismic records of chemical explosions in 1997-2000 on the former Semipalatinsk Test Site, in: *Geophysics and Non-Proliferation problems, 2001, Kazakhstan*, V.2, NNC RK, 93–98 (in Russian).

Pinsky V. (2007). Accurate location of seismic sources with and without travel time model, in: *Earthquake monitoring and seismic hazard mitigation in Balkan countries, NATO ARW series*, edited by E. Husebye and C. Christova, Springer.

Richards, P. G. and W.-Y. Kim (2005). Equivalent volume sources for explosions at depth: theory and observations, *Bull. Seism. Soc. Am.*, Vol.95, No.2, 401–407.

Sharpe, J. A. (1942). The production of elastic waves by explosion pressure: part I, theory and empirical field observations, *Geophysics* 7: 144–154.

Springer, D.L., G. A. Pawloski, J. L. Ricca, R. F. Rohrer and D. K. Smith (2002). Seismic Source Summary for All U.S. Below-Surface Nuclear Explosions, *Bull. Seism. Soc. Am.*92: (5), 1806–1840.

Stevens, J., J. Murphy and N. Rimer (1991). Seismic source characteristics of cavity decoupled explosions in salt and tuff. *Bull. Seism. Soc. Am.*, Vol.81, No.4, 1272–1291

Stevens, J., N. Rimer, H. Xu, J. Murphy, B. Barker, S. Gibbons, C. Lindholm, F. Ringdal, T. Kvaerna, and I. Kitov (2003). Analysis and simulation of cavity-decoupled chemical explosions, in *Proceedings of the 25th Seismic Research Review—Nuclear Explosion Monitoring: Building the Knowledge Base*, LA-UR-03-6029, Vol. 1, pp. 466–475.

Stevens, J. (2006). Development and Future of Explosion Source Theory, *Abstracts of the 2006 Annual SSA meeting*, San Francisco, California, 18–22 April.